Nonrigid Patient Setup Errors in the Head-and-Neck Region

Buelent Polat, Juergen Wilbert, Kurt Baier, Michael Flentje, Matthias Guckenberger[1]

Purpose: To investigate the magnitude and clinical relevance of relative motion/nonrigid setup errors in the head-and-neck (H&N) region.
Material and Methods: Eleven patients with tumors in the H&N region were immobilized in thermoplastic head masks. Patient positioning was verified using a kilovoltage cone-beam CT (kv CBCT) prior to 100 treatment fractions. Five different regions of interest (ROIs) were selected for automatic image registration of planning CT and verification CBCT: (1) the whole volume covering planning CT and CBCT, (2) the skull, (3) the mandible, (4) C1–C3, and (5) C4–C6. Differences were calculated describing relative motion between the ROIs.
Results: The 3-D patient setup error was 3.2 mm ± 1.7 mm based on registration of the whole volume. No systematic relative motion (group mean errors < 0.5 mm and < 0.5°) between planning and treatment for any ROI was observed. Mobility was largest for the skull and the mandible relative to C4–C6 with 3-D displacements of 4.7 mm ± 2.5 mm and 4.4 mm ± 2.5 mm. Relative rotations were largest around the left-right axis (nodding) between C1–C3 and C4–C6 with maximum 11°. No time trend of relative motion was observed. Margins for compensation of relative motion ranged between 5 mm and 10 mm.
Conclusion: The simplification of the patient as a rigid body was shown to result in significant errors due to relative motion in the H&N region. Margins for compensation of relative motion exceeded margins for compensation of patient positioning errors.

Key Words: Nonrigid setup errors · Cone-beam CT · Automatic image registration · Safety margin · Head and neck tumors

Strahlenther Onkol 2007;183:506–11
DOI 10.1007/s00066-007-1747-5

Nichtrigide Lagerungsfehler von Patienten mit Kopf-Hals-Tumoren

Ziel: Untersucht wurden das Ausmaß und die klinische Relevanz nichtrigider Lagerungsfehler bei der Behandlung von Kopf-Hals-Tumoren.
Material und Methodik: Elf Patienten waren für die Strahlenbehandlung von Kopf-Hals-Tumoren mittels thermoplastischer Masken immobilisiert. Bei 100 Fraktionen wurde die Patientenpositionierung mittels eines Kilovolt-Cone-Beam-CT (kv-CBCT) kontrolliert. Die automatische Registrierung von Planungs-CT und Verifikations-CBCT basierte auf fünf verschiedenen Regionen: 1. dem gesamten Volumen von Planungs-CT und Verifikations-CBCT, 2. Schädel, 3. Unterkiefer, 4. C1–C3 und 5. C4–C6. Die Unterschiede zwischen den Registrierungen beschrieben das Ausmaß der Relativbewegungen im Kopf-Hals-Bereich.
Ergebnisse: Der dreidimensionale Lagerungsfehler, basierend auf Region 1 (gesamtes Volumen), betrug 3,2 mm ± 1,7 mm. Für keine der anatomischen Regionen wurde eine systematische Relativbewegung zwischen Planung und Behandlung festgestellt (< 0,5 mm und < 0,5°). Am größten war die Beweglichkeit des Schädels und des Unterkiefers relativ zur kaudalen Halswirbelsäule: 4,7 mm ± 2,5 mm und 4,4 mm ± 2,5 mm. Rotationsbewegungen waren zwischen kranialer und kaudaler Halswirbelsäule am größten: maximal 11° um die Links-rechts-Achse (Nickbewegung). Ein zeitlicher Trend der Relativbewegungen wurde nicht beobachtet. Sicherheitssäume von 5–10 mm waren zur Kompensation dieser Relativbewegungen notwendig.
Schlussfolgerung: Substantielle Relativbewegungen im Kopf-Hals-Bereich widerlegen ein rigides Patientenmodell. Sicherheitssäume von 5–10 mm zur Kompensation dieser Relativbewegungen verdeutlichen die klinische Relevanz.

Schlüsselwörter: Nichtrigide Lagerungsfehler · Cone-Beam-CT · Automatische Bildregistrierung · Sicherheitssäume · Kopf-Hals-Tumoren

[1] Department of Radiation Oncology, Julius Maximilians University, Wuerzburg, Germany.

Received: March 2, 2007; accepted: June 28, 2007

Introduction

Multiple studies reported patient setup errors in the head-and-neck (H&N) region using different types of immobilization devices [12]. Based on these data safety margins of 3–5 mm are considered a standard in the H&N region [1, 9, 11, 20]. However, patient position was usually verified with electronic portal images (EPID). With X-ray energy in the therapeutic range of MV the contrast of these images is poor making evaluation difficult and resulting in significant variability of interpretation [14, 21].

As soft-tissue tumors themselves are not visible in the EPID, the bony anatomy is used as a surrogate. In the treatment of H&N tumors a close relation between the tumor and the bony anatomy justifies this approach. However, the selection of the appropriate bony landmark often struggles between close as possible location to the tumor and clear visibility in the EPID. This is of major importance, as the assumption of the patient as a rigid model is certainly wrong: relative motion of different anatomic regions independently of each other in the H&N anatomy is a known problem. Individual bony structures are certainly rigid objects; however, the complex anatomy of the entire H&N region has to be considered a nonrigid object. Quantifying these nonrigid setup errors based on the analysis of 2-D images is difficult which explains the lack of data on this subject in the literature.

This study investigated the magnitude of relative motion of different bony anatomic landmarks in the H&N region. The analysis was based on kilovoltage cone-beam CT (kV CBCT) studies acquired for verification of the patient setup. The clinical significance of nonrigid setup errors was estimated by means of calculation of safety margins.

Material and Methods

Eleven consecutive patients treated for tumors in the H&N region were included into this analysis. All patients were immobilized in thermoplastic head masks (Reuther, Koblenz, Germany; Figure 1). Patients were treated at an Elekta Synergy S™ (Elekta, Crawley, UK) equipped with a kV source and a digital aSi flat-panel. This allows imaging with the patient in treatment position – no movement of either the patient or the treatment couch is necessary [5, 6].

A 205° rotation of the kV source with acquisition of ~360 projections was standard protocol for acquisition of a CBCT in the H&N region. For verification of the patient setup an automatic registration (correlation coefficient algorithm) of the planning CT study and the verification CBCT was done (Elekta XVI software™) [16]. Errors were calculated in six degrees of freedom (three translations and three rotations). The treatment isocenter was defined as the correction reference point and, thus, all errors referred to this point.

A so-called alignment box defined the region of interest (ROI) for this automatic image registration: only the volume within this box was considered for the image registration. Five different ROI boxes were selected (Figure 2): (1) the whole

Figure 1. Thermoplastic head mask for positioning and immobilization of the patient. Room lasers were aligned with marks on the mask, no additional marks on shoulders or chest were used.

Abbildung 1. Thermoplastische Kopfmaske zur Positionierung und Immobilisation der Patienten. Die Patienten wurden anhand von Anzeichnungen auf der Maske an den Raumlasern ausgerichtet. Auf der Schulter oder dem Thorax waren keine zusätzlichen Anzeichnungen.

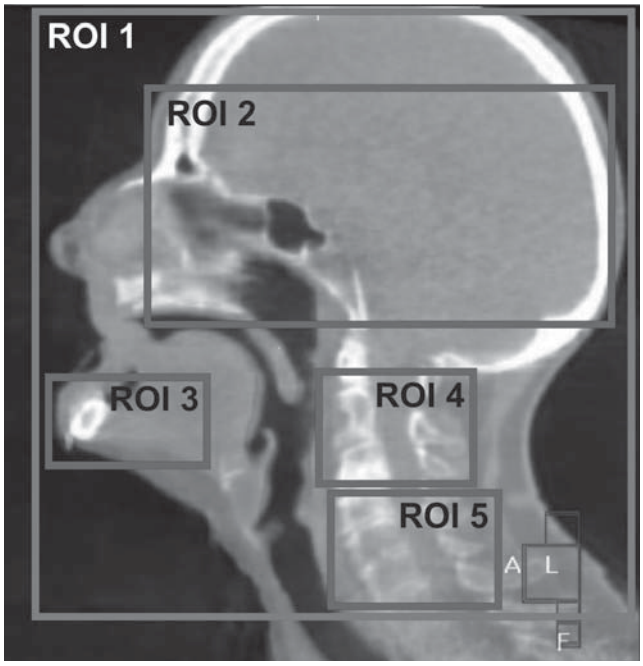

Figure 2. Five different regions of interest (ROIs) were selected for automatic image registration of planning CT and CBCT: (1) the whole volume covering planning CT and CBCT, (2) the skull, (3) the mandible, (4) C1–C3, and (5) C4–C6.

Abbildung 2. Die automatische Registrierung von Planungs-CT und Verifikations-CBCT basierte auf fünf verschiedenen Regionen (ROIs): 1. dem gesamten Volumen von Planungs-CT und Verifikations-CBCT, 2. Schädel, 3. Unterkiefer, 4. C1–C3 und 5. C4–C6.

volume covering both planning CT and CBCT, (2) the skull including the base of the skull, (3) the mandible, (4) the cranial part of the cervical spine (C1–C3), and (5) the caudal part of the cervical spine (C4–C6). In left-right direction the whole skull was included into each ROI. For a total of 100 treatment fractions the image registration between planning CT and CBCT was based on these five ROIs resulting in 500 setup errors in six degrees of freedom. Differences between registrations based on the five ROIs were calculated for evaluation of nonrigid patient positioning errors.

Errors are reported as described by van Herk [22]: for each patient the mean (systematic error) and standard deviation (SD; random error) of all errors during treatment were calculated. The group mean error (M) is defined as the average of all systematic errors; Σ is defined as the SD of the systematic errors. The root-mean-square of the random errors was calculated as σ. Errors were calculated separately for all three axes: left-right (LR), superior-inferior (SI), and anterior-posterior (AP). The length of the 3-D translational vector was calculated from errors in SI, AP, and LR direction. Safety margins for compensation of rigid and nonrigid setup errors were calculated using the formula $2.5\,\Sigma + 0.7\,\sigma$.

Table 1. Patient setup errors with registration of planning CT and cone-beam CT (CBCT) based on the region of interest (ROI) 1 (whole volume of planning CT and CBCT). Left-right (LR), superior-inferior (SI), anterior-posterior (AP), group mean error (M), standard deviation (SD) of systematic errors (Σ), root-mean-square of random errors (σ).

Tabelle 1. Lagerungsfehler der Patienten, basierend auf Registrierung von Region 1 (gesamtes Volumen von Planungs-CT und Verifikations-Cone-Beam-CT). Links-rechts (LR), superior-inferior (SI), anterior-posterior (AP).

	Translations (mm)			Rotations (°)		
	LR	SI	AP	LR	SI	AP
M	0.0	−0.5	−0.8	−0.1	−0.1	−0.4
Σ	1.6	1.3	1.6	0.8	1.5	1.3
σ	2.1	1.4	1.6	1.1	1.2	1.1

Table 2. Variation of setup errors due to relative motion of the anatomic landmarks. Standard deviation (SD) and range of setup errors within each fraction were calculated. Displayed are mean values ± SD for all fractions/patients. Left-right (LR), superior-inferior (SI), anterior-posterior (AP).

Tabelle 2. Streuung der Lagerungsfehler, bedingt durch Relativbewegungen. Bei jeder Behandlungsfraktion wurden die Standardabweichung (SD) und die Spanne der Lagerungsfehler, basierend auf den fünf anatomischen Regionen, berechnet. Dargestellt sind Mittelwert ± SD für alle Fraktionen/Patienten. Links-rechts (LR), superior-inferior (SI), anterior-posterior (AP).

	Translations (mm)			Rotations (°)		
	LR	SI	AP	LR	SI	AP
SD	1.5 ± 1.1	1.1 ± 0.6	1.5 ± 1.0	1.2 v 0.7	0.9 ± 0.6	0.9 ± 0.7
Range	3.6 ± 2.6	2.7 ± 1.4	3.5 v 2.3	3.0 v 1.9	2.2 v 1.5	2.2 ± 1.6

For statistical analysis Statistica 6.0 (Statsoft, Tulsa, OK, USA) was utilized. Differences were considered significant for $p < 0.05$. Student's t-test was used for testing differences between two groups/variables.

Results

Patient setup errors based on the registration of the whole volume covering planning CT and CBCT are shown in Table 1. These setup errors are termed "rigid setup errors" in further part of the study. The 3-D displacement vector was 3.2 mm ± 1.7 mm (mean ± SD) and the maximum error was 9.1 mm. These errors were corrected online prior to treatment in clinical practice. Margins ranging from 4.2 mm in SI direction to 5.5 mm in LR direction were calculated for compensation of these setup errors.

The SD of the setup errors based on the five ROIs was calculated for each fraction, separately for all three directions/rotations. Additionally, the maximum range of setup errors (difference between maximum and minimum error) within each fraction was calculated. These numbers describe the variation of setup errors due to the definition of different ROIs for image registration. Results are shown in Table 2. In general, variation of setup errors was significantly larger in AP and LR direction compared to SI direction ($p < 0.01$). Largest differences regarding rotational errors were seen around the LR axis ($p < 0.05$).

Differences between setup errors were calculated for describing the relative motion of the four anatomic landmarks, the deformation in the H&N region. There was no systematic relative motion between planning and treatment for any ROI: the group mean error was < 0.5 mm and < 0.5° for all directions and rotations around all axes, respectively. The motion of the mandible and the skull relative to the caudal cervical spine was significantly larger compared to the relative mobility of the other ROIs (Figure 3): the 3-D relative motion was 4.7 mm ± 2.5 mm and 4.4 mm ± 2.5 mm on average, respectively. The maximum relative motion was seen between the skull and the caudal spine with 15.5 mm. Rotations were largest between the cranial and the caudal spine: rotations around the LR axis were measured with $\Sigma = 2.4°$ and $\sigma = 1.7°$, maximum 11°. No time trend of relative motion during treatment was observed in this study: the 3-D vectors of relative motion were not different between the first and the second half of the treatment.

Differences between the registration based on the whole volume covering CBCT and planning CT and the registration based on the four anatomic landmarks were calculated. The differences describe residual errors of an IGRT (image-guided radiotherapy) correction protocol due to nonrigid setup errors separately for the four anatomic landmarks. Largest discrepancies were observed for the caudal cervical spine with 3.7 mm ± 2.4 mm. Detailed results are shown in Table 3. Margins were calculated for compensation of these errors. These margins only compensate errors due to relative motion within the H&N region, errors due to rigid patient setup errors

were not considered in this analysis. Smallest margins were calculated for the skull, largest margins for the caudal cervical spine (Table 3).

We simulated two treatments (daily imaging and online correction of errors) of advanced stage of nasopharyngeal cancer (invasion of the base of the skull) and of cancer of the floor of the mouth. In clinical practice the positioning would be based on the skull/upper cervical spine for nasopharyngeal cancer. For cancer of floor of the mouth the cervical spine would be the anatomic landmark. The margins for compensation of relative motion were calculated. Image guidance based on the skull as anatomic landmark would require margins of

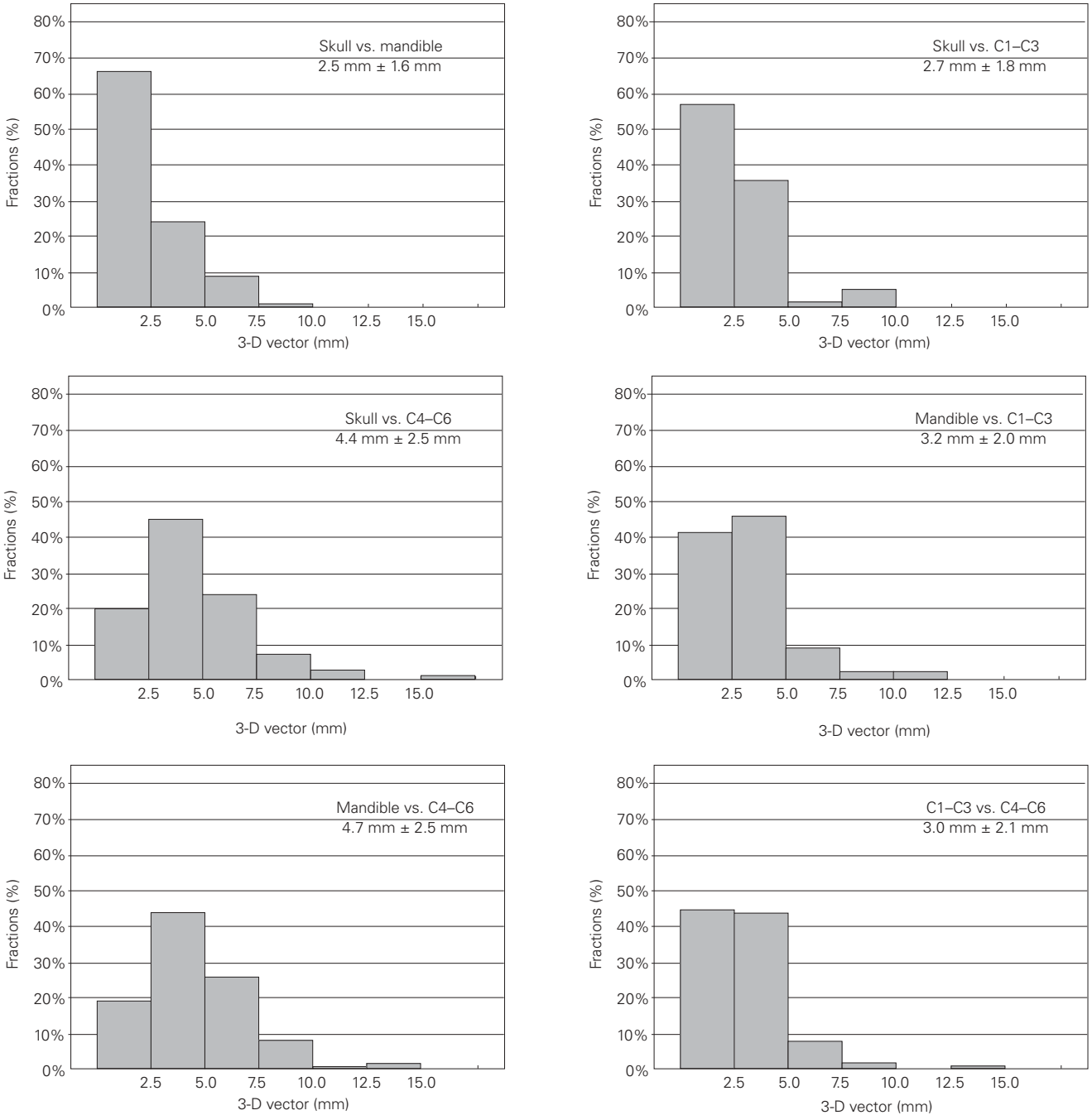

Figure 3. Relative motion (nonrigid 3-D setup errors) between the skull, the mandible, C1–C3, and C4–C6.

Abbildung 3. Häufigkeitsverteilungen der Relativbewegungen (3-D-Vektoren) von Schädel, Unterkiefer, kranialer und kaudaler Halswirbelsäule.

Table 3. Errors (mean ± SD) due to relative motion in image-guided radiotherapy (IGRT) based on the whole volume covering planning CT and cone-beam CT. Margins for compensation of relative motion were calculated. Left-right (LR), superior-inferior (SI), anterior-posterior (AP).

Tabelle 3. Fehler eines IGRT-Behandlungsprotokolls, basierend auf Region 1 (gesamtes Volumen von Planungs-CT und Verifikations-Cone-Beam-CT), durch Relativbewegungen im Kopf-Hals-Bereich. Berechnet wurden die Sicherheitssäume zur Kompensation dieser Relativbewegungen. Links-rechts (LR), superior-inferior (SI), anterior-posterior (AP).

	3 D error (mm)	Margin (mm)		
		LR	SI	AP
Skull	1.1 ± 1.4	2.2	2.3	2.3
C1–C3	2.0 ± 2.1	4.0	2.5	5.0
C4–C6	3.7 ± 2.4	6.4	4.0	7.4
Mandible	2.1 ± 1.4	2.7	4.1	4.7

7 mm (LR 9.4 mm; SI 5.2 mm; AP 7 mm) around the lower cervical lymphatics (level IV) for compensation of nonrigid setup errors. In the case of cancer of the floor of the mouth, margins of 8 mm (LR 9.5 mm; SI 6.1 mm; AP 7.1 mm) around the primary tumor would be necessary for compensation of motion relative to the landmark of the cervical spine.

Discussion

In this study we demonstrated clinically significant relative motion/deformation within the H&N region. Highest mobility was observed for the skull and for the mandible relative to the caudal cervical spine with displacements up to 15 mm and up to 11°. Rotations between the skull und the cervical spine were largest around the LR axis indicating substantial "nodding" within the thermoplastic head masks.

Inappropriate patient positioning in the thermoplastic masks does not explain these substantial nonrigid setup errors. Based on registration of the whole volume covering CBCT and planning CT the 3-D setup error was measured with 3.2 mm ± 1.7 mm. This is in very good agreement with data from the literature [12]. Margins of about 5 mm were calculated for compensation of these errors which is considered a standard in the H&N region.

Boda-Heggemann et al. reported setup accuracy using similar thermoplastic head masks [3]. With CBCT for verification significantly larger setup errors were observed in the neck compared to the skull: 7.3 mm versus 4.7 mm. This indicates substantial relative motion between the skull and the cervical spine. Zhang et al. reported setup errors for patients treated in the H&N region [23]. An in-room CT scanner was used for imaging. Variations of setup errors in the range of 10 mm between C2 and C6 vertebral bodies and the palatine process were observed.

Though correction of patient setup errors in six degrees of freedom has been described [7], such procedures are based on a rigid model of the patient. Assuming an online correction protocol with daily 3-D imaging and correction of setup errors in six degrees of freedom, the elimination of errors due to relative motion by means of image guidance is not possible. Margin calculations in our study demonstrated the potential clinical significance of relative motion within the H&N region. For compensation of setup errors based on a rigid patient model, safety margins of about 5 mm were calculated. Safety margins up to 10 mm were necessary for compensation of relative motion.

Consequently, future research should aim at reducing this significant source of error. Though multiple positioning and immobilization devices have been described for the H&N region in the literature [4], data about the potential to minimize relative motion is missing. The use of a mouthpiece might reduce mobility between the skull and the mandible. Thermoplastic masks including the skull, neck and shoulders might minimize relative motion of the caudal cervical spine. These are theoretical considerations which need to be investigated in clinical studies.

Barker et al. observed a continuous shrinkage of the primary tumor and of lymph node metastases during the course of fractionated treatment for H&N cancer [2]: the volume of the macroscopic tumor decreased by 1.8% per treatment day. Decreased coverage of the target volume and increased doses to critical structure might be the consequence. In treatment with intensity-modulated radiotherapy (IMRT), where sharp dose gradients between the target and organs at risk require high precision of treatment [10, 15, 17–19], replanning has been demonstrated to compensate these adverse effects of tumor shrinkage [8, 13]. In-room imaging with soft-tissue contrast will allow us to observe such changes during radiotherapy and select patients in whom replanning might be necessary.

Especially for patients with large tumor masses such tumor shrinkage or weight loss during radiotherapy will additionally result in loosening of the immobilization device. Increasing relative motion during the course of radiotherapy will be the consequence. This is one more reason suggesting that replanning with a new head mask might be beneficial in this collective of patients. In our study, we did not observe a time trend of nonrigid setup errors: relative mobility was not increased in the second half of the treatment. This is explained by the fact that the volume of the primary tumor and of lymph node metastases was small for all patients.

Conclusion

Substantial relative mobility within the H&N region was observed in this study. Motion of the mandible and the skull relative to the cervical spine was clinically significant: safety margins for compensation of relative mobility exceeded margins for compensation of rigid setup errors.

References

1. Astreinidou E, Bel A, Raaijmakers CP, et al. Adequate margins for random setup uncertainties in head-and-neck IMRT. Int J Radiat Oncol Biol Phys 2005;61:938–44.

2. Barker JL Jr, Garden AS, Ang KK, et al. Quantification of volumetric and geometric changes occurring during fractionated radiotherapy for head-and-neck cancer using an integrated CT/linear accelerator system. Int J Radiat Oncol Biol Phys 2004;59:960–70.
3. Boda-Heggemann J, Walter C, Rahn A, et al. Repositioning accuracy of two different mask systems-3D revisited: comparison using true 3D/3D matching with cone-beam CT. Int J Radiat Oncol Biol Phys 2006;66:1568–75.
4. Engelsman M, Rosenthal SJ, Michaud SL, et al. Intra- and interfractional patient motion for a variety of immobilization devices. Med Phys 2005; 32:3468–74.
5. Guckenberger M, Flentje M. Intensity-modulated radiotherapy (IMRT) of localized prostate cancer. A review and future perspectives. Strahlenther Onkol 2007;183:57–62.
6. Guckenberger M, Meyer J, Vordermark D, et al. Magnitude and clinical relevance of translational and rotational patient setup errors: a cone-beam CT study. Int J Radiat Oncol Biol Phys 2006;65:934–42.
7. Guckenberger M, Meyer J, Wilbert J, et al. Precision of image-guided radiotherapy (IGRT) in six degrees of freedom and limitations in clinical practice. Strahlenther Onkol 2007;183:307–13.
8. Hansen EK, Bucci MK, Quivey JM, et al. Repeat CT imaging and replanning during the course of IMRT for head-and-neck cancer. Int J Radiat Oncol Biol Phys 2006;64:355–62.
9. Hoeller U, Biertz I, Flinzberg S, et al. Hyperfractionated-accelerated radiotherapy followed by radical surgery in locally advanced tumors of the oral cavity. Strahlenther Onkol 2006;182:157–63.
10. Hong TS, Tome WA, Chappell RJ, et al. The impact of daily setup variations on head-and-neck intensity-modulated radiation therapy. Int J Radiat Oncol Biol Phys 2005;61:779–88.
11. Humphreys M, Guerrero Urbano MT, Mubata C, et al. Assessment of a customised immobilisation system for head and neck IMRT using electronic portal imaging. Radiother Oncol 2005;77:39–44.
12. Hurkmans CW, Remeijer P, Lebesque JV, et al. Set-up verification using portal imaging; review of current clinical practice. Radiother Oncol 2001; 58:105–20.
13. Kuo YC, Wu TH, Chung TS, et al. Effect of regression of enlarged neck lymph nodes on radiation doses received by parotid glands during intensity-modulated radiotherapy for head and neck cancer. Am J Clin Oncol 2006;29:600–5.
14. Lewis DG, Ryan KR, Smith CW. Observer variability when evaluating patient movement from electronic portal images of pelvic radiotherapy fields. Radiother Oncol 2005;74:275–81.
15. Manning MA, Wu Q, Cardinale RM, et al. The effect of setup uncertainty on normal tissue sparing with IMRT for head-and-neck cancer. Int J Radiat Oncol Biol Phys 2001;51:1400–9.
16. Meyer J, Wilbert J, Baier K, et al. Positioning accuracy of cone-beam computed tomography in combination with a HexaPOD robot treatment table. Int J Radiat Oncol Biol Phys 2007;67:1220–8.
17. Milker-Zabel S, Zabel-du Bois A, Huber P, et al. Fractionated stereotactic radiation therapy in the management of benign cavernous sinus meningiomas. Long-term experience and review of the literature. Strahlenther Onkol 2006;182:635–40.
18. Studer G, Lutolf UM, Davis JB, et al. IMRT in hypopharyngeal tumors. Strahlenther Onkol 2006;182:331–5.
19. Studer G, Studer SP, Zwahlen RA, et al. Osteoradionecrosis of the mandible: minimized risk profile following intensity-modulated radiation therapy (IMRT). Strahlenther Onkol 2006;182:283–8.
20. Suzuki M, Nishimura Y, Nakamatsu K, et al. Analysis of interfractional set-up errors and intrafractional organ motions during IMRT for head and neck tumors to define an appropriate planning target volume (PTV)- and planning organs at risk volume (PRV)-margins. Radiother Oncol 2006;78:283–90.
21. Van de Steene J, Van den Heuvel F, Bel A, et al. Electronic portal imaging with on-line correction of setup error in thoracic irradiation: clinical evaluation. Int J Radiat Oncol Biol Phys 1998;40:967–76.
22. Van Herk M. Errors and margins in radiotherapy. Semin Radiat Oncol 2004; 14:52–64.
23. Zhang L, Garden AS, Lo J, et al. Multiple regions-of-interest analysis of setup uncertainties for head-and-neck cancer radiotherapy. Int J Radiat Oncol Biol Phys 2006;64:1559–69.

Address for Correspondence
Dr. Matthias Guckenberger
Department of Radiation Oncology
Julius Maximilians University
Josef-Schneider-Straße 11
97080 Würzburg
Germany
Phone (+49/931) 201-28891, Fax -28221
e-mail: guckenberger_m@klinik.uni-wuerzburg.de